

Quantum Monte Carlo Analysis of Exchange and Correlation in the Strongly Inhomogeneous Electron Gas

Maziar Nekovee,^{1,*} W. M. C. Foulkes,¹ and R. J. Needs²

¹ *The Blackett Laboratory, Imperial College, Prince Consort Road, London SW7 2BZ, UK*

² *Cavendish Laboratory, Madingley Road, Cambridge CB3 0HE, UK*

(November 17, 2018)

We use variational quantum Monte Carlo to calculate the density-functional exchange-correlation hole n_{xc} , the exchange-correlation energy density e_{xc} , and the total exchange-correlation energy E_{xc} , of several electron gas systems in which strong density inhomogeneities are induced by a cosine-wave potential. We compare our results with the local density approximation and the generalized gradient approximation. It is found that the nonlocal contributions to e_{xc} contain an energetically significant component, the magnitude, shape, and sign of which are controlled by the Laplacian of the electron density.

PACS: 71.15.Mb, 71.10.-w, 71.45.Gm

Kohn-Sham density-functional theory (DFT) [1] shows that it is possible to calculate the ground-state properties of interacting many-electron systems by solving only one-electron Schrödinger-like equations. The results are exact in principle, but in practice it is necessary to approximate the unknown exchange and correlation (XC) energy functional, $E_{xc}[n(\mathbf{r})]$, which expresses the many-body effects in terms of the electron density $n(\mathbf{r})$. The current popularity of density-functional methods in condensed matter physics, quantum chemistry, and materials science reflects the remarkable success of fairly simple approximate XC energy functionals.

In the local density approximation (LDA), the XC hole n_{xc} about an electron at \mathbf{r} is assumed to be the same as in a uniform electron gas of fixed density $n = n(\mathbf{r})$. This works surprisingly well, even though real solids and molecules have strongly inhomogeneous electron densities. Almost all attempts to go beyond the LDA have been based on studies of XC in the weakly inhomogeneous electron gas. The widely used generalized gradient approximation (GGA) [2–4] incorporates information about first-order gradient corrections to the LDA, as obtained in the limit of slowly varying electron densities. This is done in a controlled way such that, for example, n_{xc} satisfies known sum rules [2], but without any guidance from the behavior of n_{xc} in the strongly inhomogeneous regime. This may explain why current GGAs, although better than the LDA, are not consistently able to deliver the very high accuracy of ~ 0.1 eV required to study many chemical reactions. To provide a new direction in the search for more accurate and reliable approximate functionals, we have used variational quantum Monte Carlo (VMC) [5] to explore exchange and correlation in the strongly inhomogeneous electron gas.

In this letter we calculate the central quantities in DFT: the XC hole n_{xc} , the XC energy density e_{xc} , and the total XC energy E_{xc} . We study an electron gas of average density n^0 corresponding to $r_s=2$ and induce strong inhomogeneities by applying a cosine-wave poten-

tial $V_q \cos(\mathbf{q} \cdot \mathbf{r})$. Fixing V_q at $2.08\epsilon_F^0$, we consider several values of $q \leq 2.17k_F^0$, where ϵ_F^0 and k_F^0 are the Fermi energy and wave vector of a uniform electron gas with $r_s=2$.

The electron density in our systems varies strongly and rapidly on the scale of the inverse local Fermi wavevector $k_F(\mathbf{r})^{-1} = (3\pi^2 n(\mathbf{r}))^{-1/3}$, producing a strikingly nonlocal behavior of n_{xc} that cannot be described by semilocal corrections to the LDA. We show, however, that the resulting LDA errors in e_{xc} have a dominant and energetically significant component, the magnitude, shape, and sign of which are controlled by $\nabla^2 n(\mathbf{r})$. The GGA is unable to correct the LDA errors in E_{xc} resulting from this component in an adequate way, a deficiency that severely restricts its accuracy. The relevance of Laplacian terms has been pointed out previously [6–8], but our calculations provide the first quantitative evidence of their importance in strongly inhomogeneous systems and for e_{xc} .

The starting point of our calculations is the adiabatic connection formula [9]. In Hartree atomic units ($e = m = 4\pi\epsilon_0 = \hbar = 1$), this expresses $E_{xc}[n]$ as the volume integral of an XC energy density e_{xc} defined by:

$$e_{xc}(\mathbf{r}, [n]) = \frac{1}{2} \int d\mathbf{r}' \frac{n(\mathbf{r})n_{xc}(\mathbf{r}, \mathbf{r}')}{|\mathbf{r} - \mathbf{r}'|}, \quad (1)$$

where n_{xc} is the coupling-constant-averaged XC hole. The definition of e_{xc} used in the construction of the GGA differs from ours by an integration by parts that does not affect the integrated E_{xc} . We favor Eq. (1), however, because of its clear physical interpretation and because it aids comparison with the LDA XC energy density, which is constructed from an approximate hole.

The XC hole n_{xc} is obtained via a coupling-constant integration,

$$\begin{aligned} & n(\mathbf{r})n(\mathbf{r}') + n(\mathbf{r})n_{xc}(\mathbf{r}, \mathbf{r}') \\ &= \int_0^1 d\lambda \langle \Psi_\lambda | \sum_i \sum_{j(\neq i)} \delta(\mathbf{r} - \mathbf{r}_i) \delta(\mathbf{r}' - \mathbf{r}_j) | \Psi_\lambda \rangle, \quad (2) \end{aligned}$$

where Ψ_λ is the antisymmetric ground state of the Hamiltonian $\hat{H}^\lambda = \hat{T} + \lambda\hat{V}_{ee} + \hat{V}^\lambda$ associated with coupling constant λ . Here \hat{T} and \hat{V}_{ee} are the operators for the kinetic and electron-electron interaction energies, and $\hat{V}^\lambda = \sum V^\lambda(\mathbf{r}_i)$ is the one-electron potential needed to hold the electron density $n^\lambda(\mathbf{r})$ associated with Ψ_λ equal to $n(\mathbf{r})$ for all values of λ between 0 and 1. At full coupling ($\lambda=1$), $V^\lambda(\mathbf{r})$ coincides with the external potential of the system. For other λ values V^λ must be determined.

Our VMC method [10] for calculating n_{xc} and e_{xc} from Eqs. (1-2) is a generalization of the scheme used by Hood *et al.* [11]. It amounts to treating *both* Ψ^λ and V^λ variationally and determining the variational parameters by simultaneously minimizing the variance of the local energy [12,13] and the deviation of n^λ from n [10]. This is achieved by adding a term proportional to $|n^\lambda - n|$ to the variance of the energy and minimizing the resulting penalty function, which attains its absolute minimum of zero only when Ψ^λ satisfies the Schrödinger equation associated with λ and $n(\mathbf{r}) = n^\lambda(\mathbf{r})$.

The VMC calculations are performed for a finite spin-unpolarized electron gas in a FCC simulation cell subject to periodic boundary conditions. We generate the ground-state density by applying the cosine-wave potential to the $\lambda=0$ system and solving the self-consistent Kohn-Sham equations within the LDA to obtain the single-particle orbitals ϕ_i . We then *define* the resulting density to be the ground-state density of the fully interacting system [14]. We consider potentials with $q = 1.11k_F^0$, $1.55k_F^0$, and $2.17k_F^0$, and cells containing 64, 78, and 69 electrons, respectively. The large amplitude of the cosine-wave potential ensures that these systems are in the strongly inhomogeneous regime, $|n(\mathbf{r}) - n^0|/n^0 \approx 1$.

The adiabatic calculations were performed using 6 equidistant values of λ in the range $[0, 1]$, and with the following Slater-Jastrow ansatz for Ψ^λ :

$$\Psi^\lambda = D^\uparrow D^\downarrow \exp \left[- \sum_{i>j} u_{\sigma_i, \sigma_j}^\lambda(r_{ij}) + \sum_i \chi^\lambda(\mathbf{r}_i) \right], \quad (3)$$

where $r_{ij} = |\mathbf{r}_i - \mathbf{r}_j|$ and D^\uparrow and D^\downarrow are spin-up and spin-down Slater determinants constructed using the exact Kohn-Sham orbitals ϕ_i . The two-body term $u_{\sigma_i, \sigma_j}^\lambda$ contained both a fixed part and a variational part as discussed in [10]. The one-body term χ^λ , the potential V^λ , and the electron density n^λ were all expanded in plane waves. At each λ we used a total of 20 variational parameters in u^λ and χ^λ and up to 7 coefficients in the plane-wave expansions of n^λ and v^λ . The optimization of the parameters in Ψ^λ and V^λ was performed using 96000 statistically uncorrelated electron configurations. This was sufficient to reduce the root mean square deviation of $n^\lambda(\mathbf{r})$ from $n(\mathbf{r})$ to less than 0.5% of $n(\mathbf{r})$ for all values of λ and all systems. After optimization, expectation values were calculated using the Monte Carlo

Metropolis method [5] with 10^6 independent configurations of all electrons. Throughout we used the modified electron-electron interaction described in [15], which virtually eliminates the finite-size errors arising from the long range of the Coulomb potential. The statistical errors were negligible except in the tails of n_{xc} in low-density regions, where they were less than 3%; this is much smaller than the differences between the VMC and LDA XC holes.

The largest systematic errors are caused by the finite size of the system and the approximate nature of Ψ^λ . These errors combine such that, even in a homogeneous electron gas, $e_{xc}^{VMC} \neq e_{xc}^{LDA}$. To circumvent this problem we performed additional VMC calculations for finite homogeneous electron gases with $N=64$ and $r_s = 0.8, 1, 2, 3, 4, 5, 8$, and 10. The results enabled us to construct a Perdew-Zunger (PZ) parameterization [16] of the VMC XC energy per electron of a finite uniform electron gas with $N=64$. This parameterization was used to calculate e_{xc}^{LDA} and e_{xc}^{GGA} in all systems studied, ensuring that these quantities were exactly equal to e_{xc}^{VMC} in any finite homogeneous system with $N=64$. This procedure largely eliminates the systematic errors in the calculated differences between e_{xc}^{VMC} and e_{xc}^{LDA} reported below.

In Fig. 1 we show snapshots of the deformation of n_{xc}^{VMC} around an electron moving in the $q=1.55k_F$ system along a line parallel to \mathbf{q} , the direction of maximum inhomogeneity, from a density maximum towards the tail of $n(\mathbf{r})$. The XC hole is plotted as a function of \mathbf{r}' around a fixed electron at \mathbf{r} , with \mathbf{r}' ranging in a plane parallel to \mathbf{q} . Also shown is the corresponding LDA hole n_{xc}^{LDA} [9]. At the density maximum (not shown) both n_{xc}^{VMC} and n_{xc}^{LDA} are centered around the electron. However, unlike n_{xc}^{LDA} , which is always spherically symmetric, n_{xc}^{VMC} is contracted in the direction of inhomogeneity and less compact. As the electron moves away from the density maximum to a point on the slope (top panel), the non-local nature of n_{xc}^{VMC} becomes manifest. While n_{xc}^{LDA} is still centered around the electron and is rather diffuse, n_{xc}^{VMC} lags behind near the density maximum and is much more compact. The nonlocal behavior of n_{xc}^{VMC} becomes remarkable at the density minimum. Here n_{xc}^{VMC} has two large nonlocal minima, each centered around a density maximum ~ 2.80 a.u. away from the electron. The LDA hole at this point is much more long ranged than n_{xc}^{VMC} and is spread over the whole system in order to satisfy the sum rule [9]: $\int d\mathbf{r}' n_{xc}^{LDA}(\mathbf{r}, \mathbf{r}') = -1$.

This striking nonlocality of n_{xc}^{VMC} also occurs in the other two systems we considered. Clearly, semilocal corrections are unable to significantly improve the LDA description of the XC hole in our systems, and fully non-local approximations are required. We found, however, that despite the strong nonlocality of n_{xc}^{VMC} , the LDA errors in e_{xc}^{VMC} can be described in terms of a semilocal quantity, the Laplacian of the electron density.

In Fig. 2 we show $e_{xc}^{LDA} - e_{xc}^{VMC}$ for two of the strongly

inhomogeneous systems studied, where e_{xc}^{LDA} is calculated using the exact ground-state density $n(\mathbf{r})$. The results are plotted along a line parallel to \mathbf{q} (we call this direction y). Also shown are $n(\mathbf{r})$ and $\nabla^2 n(\mathbf{r})$, plotted along the same line. It is apparent that the shape, magnitude, and sign of the LDA errors in e_{xc} closely follow the shape, magnitude, and sign of $\nabla^2 n(\mathbf{r})$. The LDA errors in e_{xc} are large and negative in regions where $\nabla^2 n(\mathbf{r})$ is large and negative (around density maxima), and large and positive in regions where $\nabla^2 n(\mathbf{r})$ is large and positive. The GGA XC energy density is not defined via Eq. (1) and so GGA errors are not shown.

The VMC values of the integrated E_{xc} are shown in Table I, along with the differences $\Delta E_{xc}^{LDA} = E_{xc}^{LDA} - E_{xc}^{VMC}$ and $\Delta E_{xc}^{GGA} = E_{xc}^{GGA} - E_{xc}^{VMC}$ (The version of the GGA used here is due to Perdew, Burke, and Ernzerhof [4]). The LDA errors in E_{xc} reflect the profound effect of the Laplacian errors in e_{xc} and change sign from positive (for the $q=1.11k_F^0$ system) to negative (for the two other systems) as q increases and the negative contributions to Δe_{xc} , which occur where $\nabla^2 n(\mathbf{r}) < 0$, become dominant. The GGA corrections are by construction *always* negative [2–4]; they improve E_{xc}^{LDA} for the $q=1.11k_F$ system but worsen it for the two other systems.

Since any smooth density $n(\mathbf{r})$ may be expanded as a power series, the XC energy density functional may always be written as

$$e_{xc}(\mathbf{r}, [n]) = e_{xc}(\mathbf{r}, n(\mathbf{r}), \nabla_i n(\mathbf{r}), \nabla_i \nabla_j n(\mathbf{r}), \dots). \quad (4)$$

The GGA may be viewed as an attempt to approximate the right-hand side of Eq. (4) as a nonlinear function of $n(\mathbf{r})$ and $\nabla_i n(\mathbf{r})$. In the case of the exchange energy, a uniform scaling argument [17] shows that

$$e_x = F_x(p, l, \dots) e_x^{LDA}, \quad (5)$$

where F_x is an enhancement factor, e_x^{LDA} is the LDA exchange energy density, and $p = |\nabla n|/(2k_F(\mathbf{r})n(\mathbf{r}))$ and $l = \nabla^2 n/(4k_F^2(\mathbf{r})n(\mathbf{r}))$ are a dimensionless gradient and a dimensionless Laplacian, respectively. We have calculated F_x exactly for our systems and investigated its dependence on p and l . Figs. 3a and 3b are scatter plots showing values of F_x plotted against values of p and l , respectively.

The two-valued nature of Fig. 3a arises because the mapping from density gradient to position is two valued in our systems. For example, the density gradient is zero both at the minimum and the maximum of the density, where the required corrections to the LDA XC hole are completely different, as can be inferred from Fig. 1. In sharp contrast, F_x is a simple and almost unique function of l . This suggests that the inclusion of Laplacian terms may allow the construction of simpler and more accurate approximate functionals. In most gradient expansions the Laplacian terms allowed by symmetry are transformed into $|\nabla n(\mathbf{r})|^2$ terms via an integration by

parts. This is only possible when the dependence on l is linear, however, which is not the case here as can be seen from Fig. 3b. Furthermore, the integration by parts destroys the physical interpretation in terms of the XC hole and so hinders further progress.

We note that there is a one-to-one relationship between position and l in our structures, and so an enhancement factor of the form $F_x(l)$ might not be as universal as Fig. 3b suggests. However, the energetic significance of the Laplacian terms, and the strong similarity between the form of the Laplacian and the LDA errors in e_{xc} (see Fig. 2), give us confidence in the physical importance of the Laplacian in describing inhomogeneity corrections to the LDA. Very recently, Becke [7] and Perdew *et al.* [8] have constructed beyond-GGA functionals that contain the reduced Laplacian as a parameter. We consider this a step in the right direction and believe that the detailed *local* information on n_{xc} and e_{xc} in the strongly inhomogeneous regime provided by our VMC calculations can be used to improve such functionals.

We thank R.Q. Hood for useful discussions, G. Rajagopal and A.J. Williamson for help with the VMC codes, and L. Smith for help with visualization. M.N. was supported by an EU Marie Curie Fellowship under Grant ERBFMBICT961736. Our calculations were performed on the CRAY-T3E at EPCC.

* Present address: Department of Chemistry, Queen Mary and Westfield College, Mile End Road, London E1 4NS, UK.

- [1] P. Hohenberg and W. Kohn, Phys. Rev. **136**, B864 (1964); W. Kohn and L. J. Sham, Phys. Rev. **140**, A1133 (1965).
- [2] J. P. Perdew and Y. Wang, Phys Rev. B **33**, 8880 (1986).
- [3] A. D. Becke, J. Chem. Phys. **98**, 5648 (1993).
- [4] J. P. Perdew, K. Burke, and M. Ernzerhof, Phys. Rev. Lett. **77**, 3865 (1996).
- [5] B. L. Hammond, W. A. Lester, Jr., and P. J. Reynolds, *Monte Carlo Methods in Ab Initio Quantum Chemistry* (World Scientific, Singapore, 1994).
- [6] E. Engel and S.H. Vosko, Phys. Rev. B **50**, 10498 (1994); C.J. Umrigar and X. Gonze, Phys. Rev. A **50**, 3827 (1994).
- [7] A.D. Becke, J. Chem. Phys. **109**, 2092 (1998).
- [8] J. P. Perdew, S. Kurth, A. Zupan, and P. Blaha, Phys. Rev. Lett. **82**, 2544 (1999).
- [9] R. G. Parr and W. Yang, *Density Functional Theory of Atoms and Molecules* (Oxford University Press, Oxford, 1988).
- [10] M. Nekovee *et al.* Adv. Quantum Chem. **33**, 189 (1999).
- [11] R. Q. Hood *et al.* Phys. Rev. Lett. **78**, 3350 (1997).
- [12] C. J. Umrigar, K. G. Wilson, and J. W. Wilkins, Phys. Rev. Lett. **60**, 1719 (1988).

- [13] A. J. Williamson *et al.* Phys. Rev. B **53**, 9640 (1996).
- [14] This has the advantage that the ϕ_i are by construction the exact Kohn-Sham orbitals for density $n(\mathbf{r})$, and their Slater determinant is the exact wave function at $\lambda=0$.
- [15] L. M. Fraser *et al.* Phys. Rev. B **53**, 1814 (1996); A. J. Williamson, *et al.* Phys. Rev. B **55**, R4851 (1997).
- [16] J. P. Perdew and A. Zunger, Phys. Rev. B **23**, 5048 (1981).
- [17] See M. Levy and J. P. Perdew, Phys. Rev. A **32**, 2010 (1985), for a derivation for the case $F_x=F_x(p)$. The generalization to the case $F_x=F_x(p, l)$ is straightforward.

TABLE I. Exchange-correlation energies (Hartrees per electron) and the LDA and GGA errors in this quantity for different values of the wave vector \mathbf{q} . The statistical errors in E_{xc}^{VMC} are indicated.

q/k_F^0	E_{xc}^{VMC}	ΔE_{xc}^{LDA}	ΔE_{xc}^{GGA}
1.11	-0.3289 ± 0.0001	$+0.0042$	$+0.0001$
1.55	-0.3127 ± 0.0001	-0.0005	-0.0074
2.17	-0.2882 ± 0.0001	-0.0066	-0.0140

FIG. 1. (color) The VMC and LDA $n_{xc}(\mathbf{r}, \mathbf{r}')$ for the $q=1.55k_F^0$ system plotted around an electron fixed at \mathbf{r} (indicated by a white bullet) with \mathbf{r}' ranging in a plane parallel to \mathbf{q} : (top) electron on the slope; (bottom) electron at a density minimum. The VMC hole is shown on the left and the LDA hole on the right. The charge density is also represented schematically. The color coding is only for n_{xc} and varies between -0.0500 (blue) and -0.0025 (red).

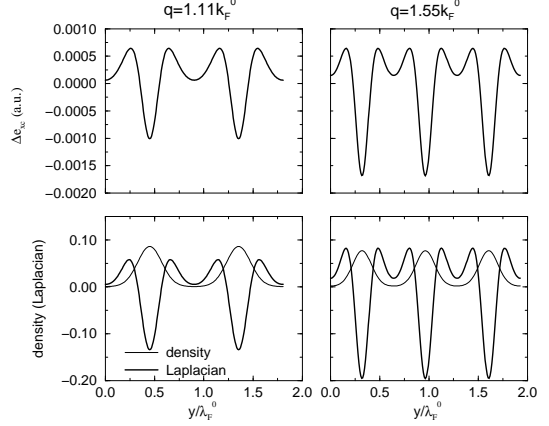


FIG. 2. The upper graphs show $e_{xc}^{LDA} - e_{xc}^{VMC}$ along a direction parallel to \mathbf{q} for two different strongly inhomogeneous systems. The lower graphs show the corresponding electron densities (light lines) and Laplacians (heavy lines). Distances are in units of the Fermi wavelength $\lambda_F^0 = 2\pi/k_F^0$.

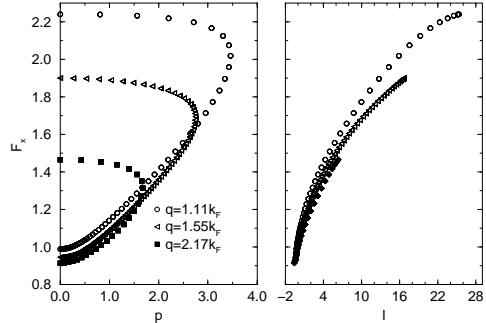


FIG. 3. The left panel plots the exact enhancement factor F_x against the reduced density gradient for three strongly inhomogeneous systems. The right panel shows the same quantity plotted against the reduced density Laplacian.

This figure "fig1.BOTTOM.jpg" is available in "jpg" format from:

<http://arxiv.org/ps/cond-mat/0008181v1>

This figure "fig1.TOP.jpg" is available in "jpg" format from:

<http://arxiv.org/ps/cond-mat/0008181v1>